

ON THE DYNAMIC PROPERTIES OF CLAY

by Sakuro MURAYAMA* and Toru SHIBATA**

Summary

In this paper, experimental and theoretical studies on the dynamic properties of undisturbed clay are reported in four articles : 1. Flow character of clay under the vibrating load, 2. Fatigue strength of clay, 3. Effect of vibration on the long-term strength of clay and 4. Effect of vibration on the shearing strength. The main results obtained here are as follows : (1) The upper yield value obtained by the dynamic flow test performed at lower side of the resonance range is equal to the value obtained by the static flow test. (2) The number of repetitions required to produce the fatigue fracture of clay is determined only by the applied repetitional maximum stress irrespective of the frequency. (3) The decreases of the long-term strength and the shearing strength by vibration, in the case of undisturbed clay, depend on the maximum acceleration of vibration.

1. Flow Character of Clay under the Vibrating Load

Apparatus, test procedures and soil tested In order to investigate the flow behaviour of clay under the vibrating load, uni-axial dynamic flow tests were performed with the apparatus shown diagrammatically in Fig. 1. As shown in this figure, vertical sinusoidal vibration produced by a two-mass oscillator is applied on the specimen. The oscillator shown in Fig. 1 has two sets of eccentric weights which are rotated in opposite directions with same phase and produce a vertical sinusoidal vibration as the unbalanced eccentric forces are mutually eliminated in all directions except vertical one. As the oscillating force can be controlled by adjusting the phase-difference of the each sets of eccentric weight on each shaft, we can change the frequency of oscillation without varying the magnitude of the dynamic force. The total dead weight of assembly of oscillator (own weight of oscillator is 4.4 kg), the base plate bolted to the bottom of the oscillator and the piston is 5.3 kg. The maximum permissible alternating force is 100 kg at a frequency of 2,760 rpm. The oscillator is driven by a 1/8 Hp AC motor through a flexible shaft.

The pressure exerted on the clay specimen by the piston consists of a static pressure equal to the dead weight of the oscillator assembly and a alternating force with a force amplitude twice of the centrifugal force of the two eccentric weights. The dynamic compression loads were so restrained as the maximum vertical stresses in the specimens to be less than the pre-consolidation stresses of the specimens to avoid the effect of consolidation. The settlement of the clay specimen was measured by a dial extensometer and vertical displacement amplitude by a hand-vibrograph.

* Dr. Eng., Professor at the Disaster Prevention Research Institute, Kyoto University, Japan ; Member of Japan Society of Civil Engineers.

** Dr. Eng., Assistant Professor at the Disaster Prevention Research Institute, Kyoto University, Japan ; Member of Japan Society of Civil Engineers.

Since even a small loss of water from the specimen would cause a substantial increase in strengths, during the uni-axial dynamic flow tests, every specimen was kept their water content unchanged by encasing the specimen in thin membrane and the covered specimens were totally immersed in water. Moreover, to avoid the effects of the stress-history given to the specimen by other test, each fresh specimen obtained from a same clay sample which had never received only other test was used for each uni-axial vibrating load.

Undisturbed clay specimens used for the dynamic flow tests were obtained from the Umeda Alluvial Clay Stratum in Osaka City by means of the thin-walled sampler with stationary piston. The sample tested had clay fraction of 53 %, a liquid limit of 95 %, a plastic limit of 30 %, and a natural water content ranging from 65 to 71 %. Most undisturbed specimens were cut in cylindrical shape of 3.5 cm in diameter and 8.0 cm long, by suitable trimming devices.

Resonant characteristics of clay Preliminary experiments were performed to measure the resonance ranges of the system consists of the oscillator assembly and clay specimen changing the frequency from a low frequency (240 cpm) to a high frequency (1,960 cpm) at a constant value of dynamic load of 20 sec duration. Longitudinal displacements of specimens and amplitudes of vibration were measured at various frequencies of vibrating load and the displacement amplitude — frequency relation curves are obtained as shown in Fig. 2, in which σ_{max} denotes the maximum intensities of vibrating stress.

It will be noted from Fig. 2 that the resonant frequency of the system increases with decreasing water content, viz. the resonant frequency appears in the neighbourhoods of 1,200 cpm for higher water content of 68.7 %, and about 1,600 cpm for lower water content of 65.8 %. It is also seen that the resonant frequency changes so slightly with the magnitude of oscillating force that the modulus of elasticity can be regarded as constant within these stress ranges.

Uni-axial dynamic flow test On the dynamic flow test, applied frequency of the vibrating load was selected not to exceeds the resonance range to avoid any magnification of the centrifugal-force values by resonance as already pointed out by G.P.Tschebotarioff (Ref. 1). Using clay samples above stated, dynamic flow tests were performed in which the uni-axial oscillating force was kept at a constant value during the test. The longitudinal deformation of specimen was measured by a dial gauge at specified time intervals after application of oscillating force. The results of tests are shown as strain — time diagrams in Fig. 3 and 4, in Fig. 4 abscissa shows elapsed time t in logarithmic scale and ordinate strain ϵ respectively.

From the strain — time curves shown in Fig. 4, the features worth noticing are as follows : (1) The dynamic flow strain ϵ increases proportionally to the logarithm of time $\log t$, if the maximum intensities of vibrating stress σ_{max} is smaller than a certain value. (2) If the maximum value of vibrating stress is larger than a certain critical value, the curves in Fig. 4 rise concave upwards and this tendency suggests the occurrence of failure in future after a certain duration of the loading.

It will be discussed in the following part of this article that the critical value coincides with the upper yield value of the clay. (3) The slopes of these lines related (1) increase with the maximum intensities of vibrating stress σ_{max} , and it will be shown that the tangent of the slope angle of each line is directly proportional to σ_{max} as shown in Fig. 5 whose ordinate and abscissa show the tangent of the slope angle of the line b and the applied stress of the curve illustrated in Fig. 4 respectively.

Next, the effect of the maximum intensity of vibrating stress σ_{max} on strain rate $d\varepsilon/dt$ are investigated. In Fig. 6 the strain rate $d\varepsilon/dt$ obtained from Fig. 3 is plotted against σ_{max} for various constant values of the time, taking the time as $t=45$ sec, 1.5 min, 2.5 min and 5.5 min. This figure shows that the curves are linear within the stress range up to $\sigma_{max}=0.72$ kg/cm² which is called the upper yield value, whereas they rise concave upwards at $\sigma_{max}>0.72$ kg/cm². Moreover, all linear parts of these curves have a tendency to concentrate at a point on the σ_{max} -axis, viz. concentrate at the lower yield value. Thus, in the dynamic case, the upper and lower yield values can be also uniquely determined by the same procedure as the static case.

Such a flow diagram obtained by the flow test by a static load on the same identical fresh undisturbed sample as used in dynamic flow test is shown in Fig. 7. From this figure, the upper and the lower yield value can be determined as 0.72 kg/cm² and 0.10 kg/cm² respectively. It will be noted that the upper yield value obtained by the dynamic flow test performed at lower side of the resonance range is equal to the value obtained by the static flow test.

2. Fatigue Strength of Clay

As already stated in Art. 1, the rate of the flow strain of clay due to the repetitional loading increases and clay will produce a fracture in future if the applied stress larger than the upper yield value. In this paper, the authors define such repetitional stress that produces a fracture the fatigue strength of clay and will determine it in connection with repetitional number.

Apparatus, test procedures and soil In order to carry out the experiments on fatigue strength of clay, two types of tests were used. (a) Slow repetitional loading test (Symbol : Sr) :— Repetitional loads of same magnitude and same loading duration were applied on the clay specimen at same interval of removal of the load by using a stress-controlled triaxial compression apparatus. Fig. 8(a) shows the schematic relation of the stress — time due to repetitional loading and σ_{max} is larger than the upper yield value of clay. In this figure, τ and τ' are duration time of loading and load-removing per one cycle of loading respectively.

(b) Quick repetitional loading test (Symbol : Qr) :— Vibrating load produced by a two-mass oscillator driven by 1/8 Hp AC motor was applied on the specimen, as shown in Fig. 1. The stress amplitude exerted on the clay specimen is shown in Fig. 8(b) and σ_{max} is adopted larger than the upper yield value of clay.

In each type of test, the relations between the fatigue strength and the number of stress cycles were obtained. The fatigue strength tests were made on undisturbed samples of two alluvial clays. One had a clay fraction of 46 %, a liquid limit of 79 %, a plastic limit of 31 % and a natural water content of 62.3 % (sample No. 1), the other clay fraction of 43 %, a liquid limit of 80 %, a plastic limit of 30 % and a natural water content of 62.0 % (sample No. 2). The undisturbed specimens were cut in cylindrical shape of 3.5 cm in diameter and 8.0 cm long.

Theoretical consideration Prior to explain the results of tests, the fatigue strength of clay is studied theoretically as follows. In the case of Fig. 8(a), the relation between the number of repetitions n and time t is represented as

$$\frac{dn}{dt} = \frac{1}{(\tau + \tau')} \dots \dots (1)$$

When τ is equal to τ' , we get the relation between dn/dt and the frequency f

$$\frac{dn}{dt} = \frac{1}{2\tau} = f \dots \dots (2)$$

On the basis of the theory of rate process (Ref. 2), the fundamental equation for the fatigue strength of clay is represented as

$$\frac{-1}{\tau \cdot N_b} \frac{dN_b}{dn} = \frac{\kappa T}{h} \exp\left(\frac{-E_0}{\kappa T}\right) \exp\left(\frac{\lambda \cdot \sigma_{max}}{2N_b \kappa T}\right) \dots \dots (3)$$

or

$$\left. \begin{aligned} -\frac{1}{N_b} \frac{dN_b}{dn} &= A \cdot \exp\left(\frac{\sigma_{max}}{B \cdot N_b}\right) \\ A &= \frac{\tau \kappa T}{h} \exp\left(\frac{-E_0}{\kappa T}\right), B = \frac{2\kappa T}{\lambda} \end{aligned} \right\} \dots \dots (4)$$

where N_b is the number of bonds per unit cross sectional area perpendicular to the direction of the applied stress of clay, κ is Boltzmann's constant, T is the absolute temperature, h is Planck's constant, E_0 is the activation free energy and σ_{max} is the applied repetitional maximum stress. The Eq. (5) representing the relation between the repetitional maximum stress σ_{max} and the number of repetitions required to produce the fatigue fracture n_f can be obtained by solving Eq. (4) assuming n becomes n_f when N_b becomes zero.

$$\sigma_{max} = B \cdot N_{b0} \left(\log \frac{1}{A} - \log n_f \right) \quad (5)$$

Eq. (5) represents the linear relation between the applied repetitional maximum stress σ_{max} which is defined as the fatigue strength and logarithm of n_f .

Analysis of data Experimental results are shown in Fig. 9 and 10, the former represents the relations of σ_{max} and $\log n_f$ obtained by Sr-test and the latter the same one obtained by Qr-test. These figures may correspond to so-called S-N curves of metals. Since the experimental $\sigma_{max} - \log n_f$ relations are linear, it can easily be seen that they are satisfactorily agree with Eq. (5) in the both cases of Sr-test and Qr-test. As the $\sigma_{max} - \log n_f$ line of Qr-tests performed at 480 cpm and 780 cpm coincide each other as shown in Fig. 10, it can be said that n_f is determined only by σ_{max} irrespective of the frequency, if the frequency of vibrating stress is less than the resonance range.

3. Effect of Vibration on the Long-term Strength of Clay

Several investigators (Ref. 3,4) showed that the lowering of the yield value of disturbed clay during vibration may depend on the acceleration of vibration. In order to know the tendency about undisturbed clay, effect of vibration on the long-term strength of clay is studied. If any constant static stress exceeding the upper yield value is applied on clay, the clay fails after it flows. Since the authors define such stress as exceeds the upper yield value the long-term strength, the long-term strength does not mean a definite value.

Apparatus, test procedures and soil The apparatus used were the same as those used for the former experiments described in Art. 1 ; the details of which are shown in Fig. 1. The oscillating force of 2.5 kg (corresponding stress amplitude : 0.26 kg/cm^2) was kept at a constant value during the test. Since the total dead weight of oscillator assembly was 5.3 kg (corresponding value of σ_{max} shown in Fig. 8(b) was equal to 0.55 kg/cm^2), the stress exerted on clay specimen σ_{max} was equal to $\sigma_{max} = 0.26 + 0.55 = 0.81 \text{ kg/cm}^2$ and this stress was adopted not to exceed the preconsolidation stress of clay specimen of 2.0 kg/cm^2 . In order to obtain the experimental relation between the long-term strength of clay during vibration and acceleration of vibration, experiments were performed under the various frequency range of vibration from 420 to 1,620 cpm. The maximum acceleration of vibration α was computed by the equation $\alpha = 4\pi^2 f^2 a$ gal, where f ; frequency (cps), a ; longitudinal displacement amplitude (cm) which was measured by a hand-vibrograph in this experiment. Under these conditions the elapsed time to failure was measured.

The undisturbed saturated sample tested had a clay fraction of 54 %, a liquid limit of 96 %, a plastic limit of 29 % and a natural water content of 68.7 %. The undisturbed specimens were cut in cylindrical shape of 3.5 cm in diameter and 8.0 cm long.

Experimental results Fig. 11(a) shows the relation of longitudinal displacement amplitude and frequency, Fig. 11(b) the relation of maximum acceleration of vibration and frequency, and Fig. 11(c) relation of the elapsed time to flow failure and frequency. It will be noted from these figures that the maximum acceleration of vibration and the elapsed time to flow failure, as well as the longitudinal displacement amplitude, show the each peak at $f = 1,140 \text{ cpm}$. Fig. 12 shows the relation of the elapsed time to flow failure under vibration $t_{f,d}$ and the maximum acceleration of vibration α plotted on semi-logarithmic paper. From this figure it is found that the decrease of the time to flow failure depends on the maximum acceleration of vibration. From Fig. 12, moreover, the value of $t_{f,d}$ corresponding to $\alpha = 0$, viz. the elapsed time to failure under a constant static load, is obtained as $t_f = 500 \text{ min}$.

In order to compare the elapsed time to failure under vibrating load with that of static case, the static long-term strength tests were performed. Fig. 13 shows the relation between the long-term strength and logarithm of the time to failure obtained by the static long-term strength test by using the same sample as used in dynamic one. From this figure the static long-term strength corresponding to $t_f = 500 \text{ min}$ is obtained as $\sigma = 0.73 \text{ kg/cm}^2$; this value of 0.73 kg/cm^2 is found to be equal to the

dynamic effective stress σ_e shown in Fig. 8(b), where σ_e is calculated as $\sigma_e = \sigma_m + (\sigma_{max} - \sigma_m)/\sqrt{2} = 0.55 + (0.81 - 0.55)/\sqrt{2} = 0.73 \text{ kg/cm}^2$. The ratios of the elapsed time to failure in dynamic case to that in static one ($t_{f,s} = 500 \text{ min}$) are plotted in Fig. 14 against the maximum acceleration of vibration on logarithmic paper. The experimental data lie on a straight line in a logarithmic scale: this means that the decrease of elapsed time to failure in dynamic case depends on the maximum acceleration of vibration.

4. Effect of Vibration on the Shearing Strength

In this article, the factors that influence the shearing strength of clay during vibration are studied.

Apparatus, test procedures and soil The direct double-shear box apparatus shown in Fig. 15 was used. The vertical vibrating load produced by a two-mass oscillator was applied on the specimen. In this case, the oscillating force of 4.4 kg (corresponding stress amplitude: 0.28 kg/cm^2 , stress produced by own weight: 0.14 kg/cm^2 , therefore $\sigma_{max} = 0.28 \text{ kg/cm}^2$, $\sigma_{min} = 0$) was kept at a constant value during the test. The shearing strength during vibration was measured by increasing the horizontal shearing force continuously at a suitable rate until the shear failure occurred. The frequency range of vertical vibration load was controlled from 576 to 2,970 cpm, and the corresponding maximum acceleration of vibration α was computed by the method as stated in Art. 3. The clay sample tested had a clay fraction of 50%, a liquid limit of 67.3%, a plastic limit of 27.3%, a natural water content of 52.3% and a preconsolidation stress of 1.8 kg/cm^2 . The undisturbed specimens were cut in prismatic shape, 4 cm square and 5.5 cm long. Water content of the specimen remains practically unchanged during the application of the vertical vibrating load and the horizontal shearing force.

Experimental results Fig. 16 shows the results of shearing tests during vibrations. In this figure, the vertical displacement amplitude, maximum acceleration of vibration and shearing strength during vibration are plotted against the frequency. It will be noted that the maximum acceleration and the shearing strength during vibration, as well as the amplitude of vibration, give their peaks at 1,680 cpm. In Fig. 17, the ratios of the shearing strength in dynamic case to that in static one are plotted against the maximum acceleration of vibration on logarithmic paper. In this test, the static shearing strength was measured under the vertical stress equal to σ_{max} . Since the relationship shown in Fig. 17 is represented by a straight line on logarithmic scale, the decrease of the shearing strength in dynamic case depends on the maximum acceleration of vibration.

References

- 1) G.P. Tschebotarioff: Soil Mechanics, Foundations and Earth Structures, Mc Graw Hill, 1953, p. 578.
- 2) S. Murayama and T. Shibata: On the Rheological Characters of Clay - Part 1, Disaster prevention Research Inst. Kyoto Univ. Bulletin No. 26, Oct., 1958.

3) T.Mogami and K.Kubo : The Behaviour of Soil during vibration,
Proc. 3rd Int. Conf. Soil Mech. and Found. Eng., Vol. 1, 1953, pp. 152 -
155.

4) S.Murayama and K.Tanimoto : Dynamical Behaviour of Foundation,
Disaster Prevention Research Inst. Kyoto Univ. Bulletin No. 8, 1954, pp.
18 - 24.

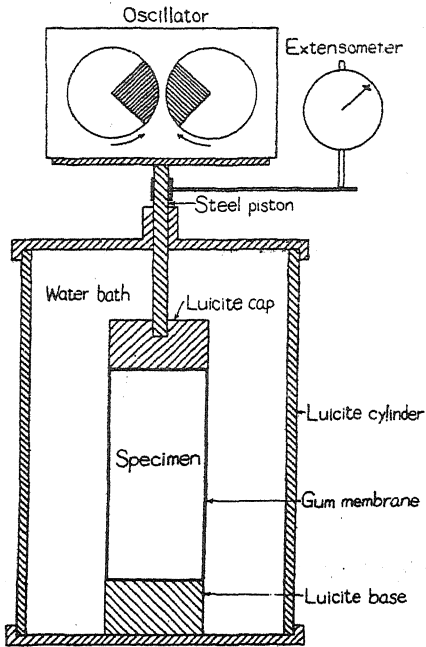


Fig. 1 Uni-axial dynamic flow apparatus.

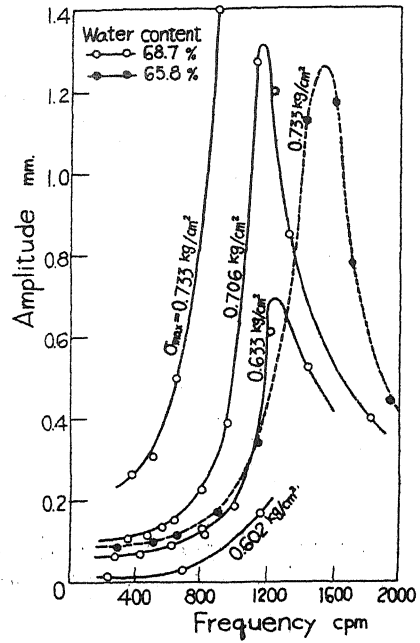


Fig. 2 Resonance curves of clay specimens under the action of vertical vibrating forces.

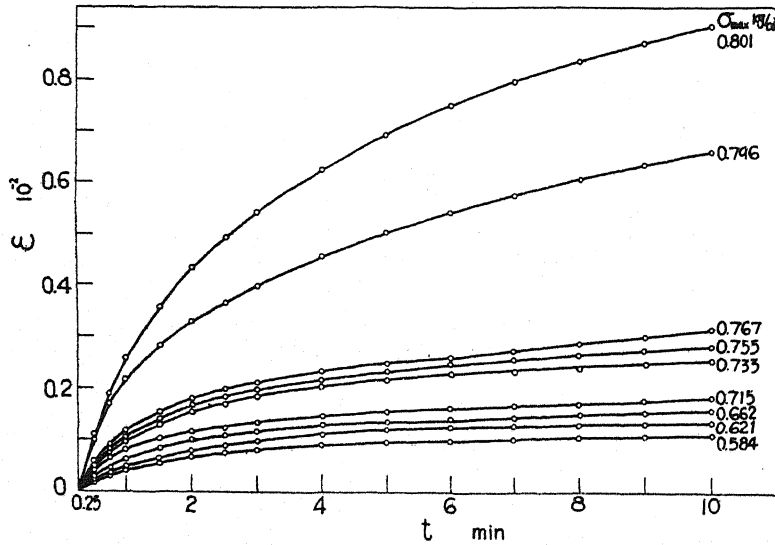


Fig. 3 General relations between dynamic flow strain ϵ and applying time with oscillating force whose maximum stress is σ_{max} .

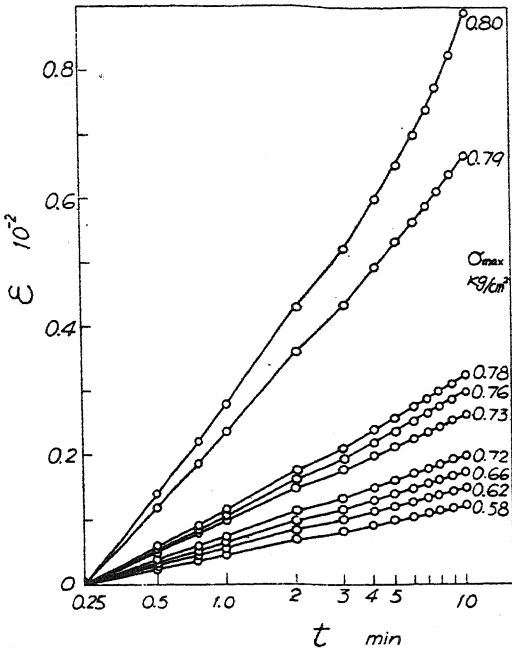


Fig. 4 Dynamic flow curves plotted on semi-logarithmic scale.

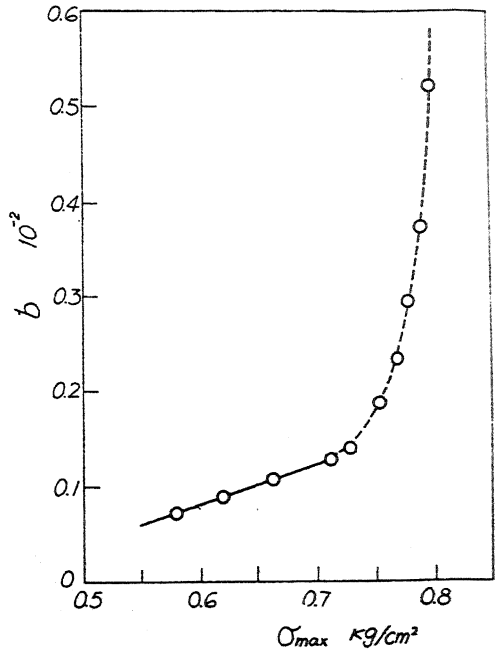


Fig. 5 Relationship between the tangent of the slope angle of dynamic flow curves plotted on semi-logarithmic scale b and σ_{max} .

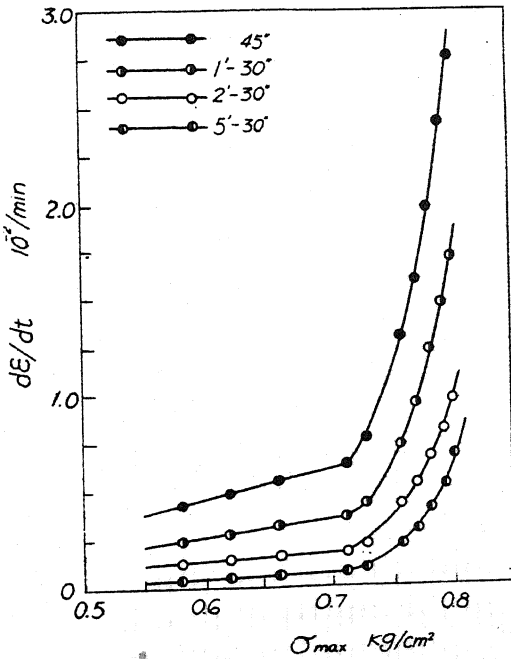


Fig. 6 Relationship between strain rate $d\epsilon/dt$ at various instants t and dynamically applied stress σ_{max} plotted from Fig. 3.

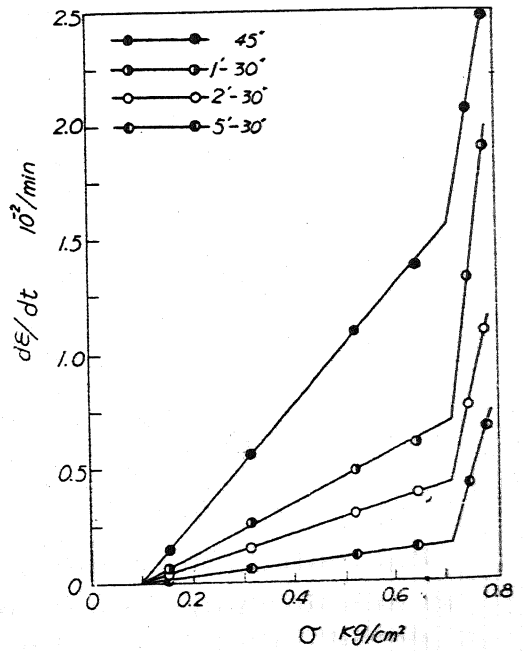


Fig. 7 Relationship between strain rate $d\epsilon/dt$ at various instants t and statically applied stress σ

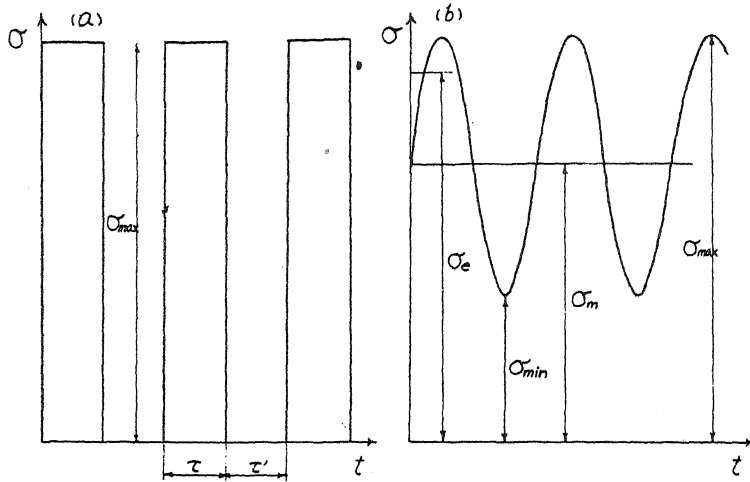


Fig. 8 Two types of loading stress applied with (a) controlled-stress tri-axial compression apparatus (b) two-mass oscillator.

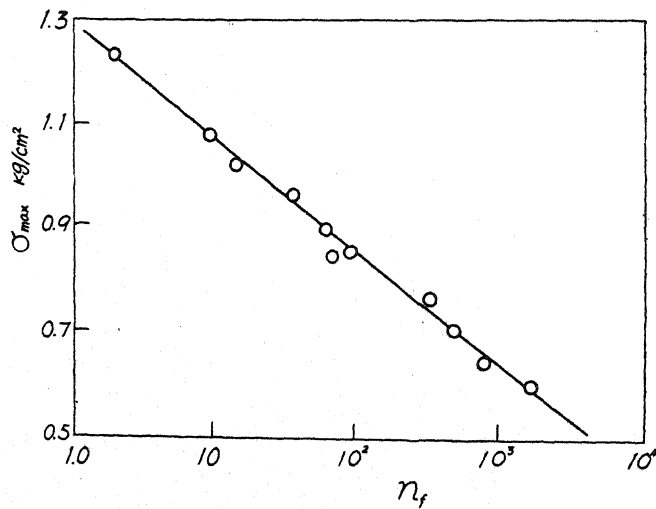


Fig. 9 Relationship between applied maximum stress σ_{max} (type of loading - (a)) and its number of repetition n_f .

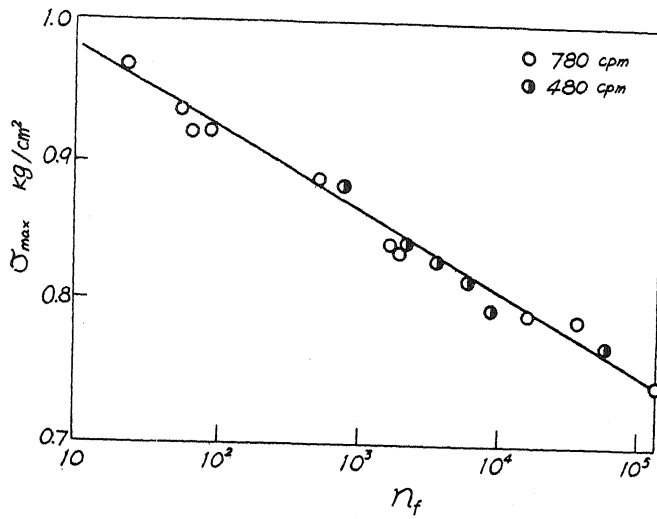


Fig. 10

Relationship between applied maximum stress σ_{max} (type of loading - (b)) and its number of repetition n_f .

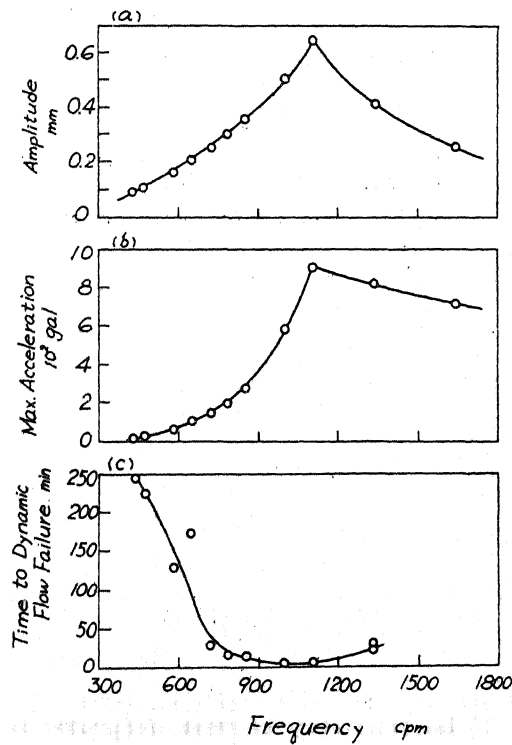


Fig. 11

Results of dynamic flow tests with clay specimens. (a) shows the relation of longitudinal displacement amplitude and frequency, (b) the relation of maximum acceleration of vibration and frequency, and (c) the relation of the elapsed time to flow failure and frequency.

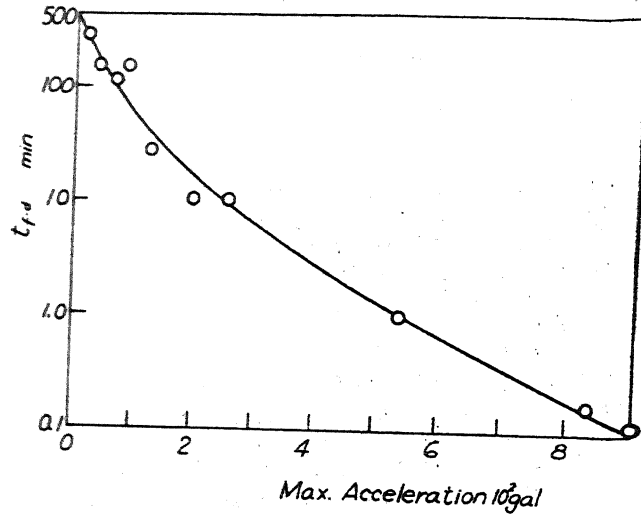


Fig. 12 Relationship between time to dynamic flow failure t_{fd} and maximum acceleration.

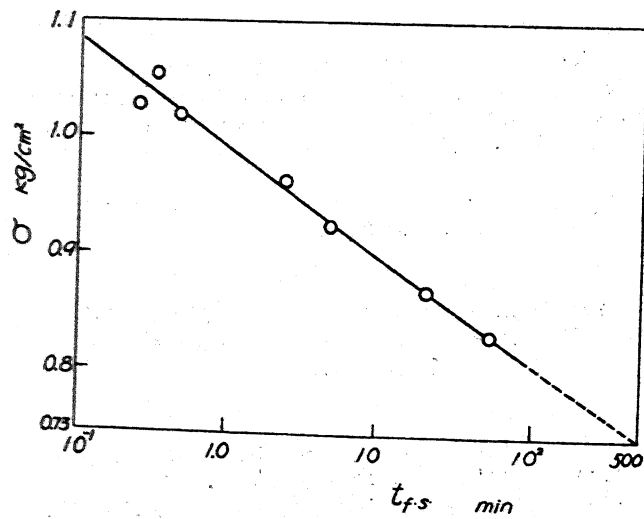


Fig. 13 Relationship between compressive strength σ and time to flow failure t_{fs} .

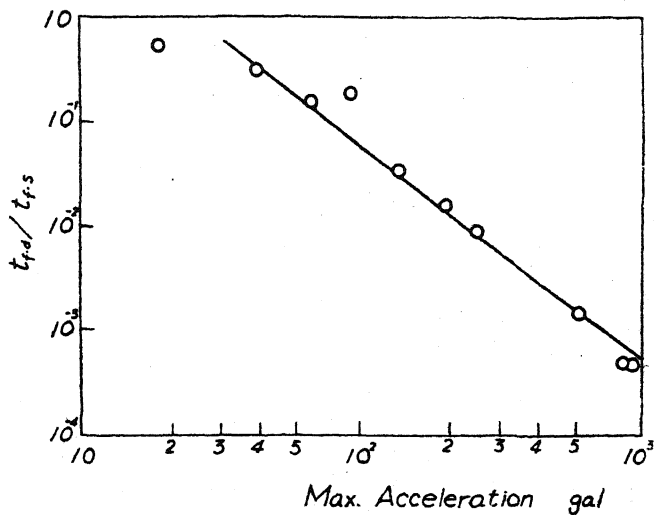


Fig. 14 Relationship between the ratio of time to flow failure $t_{f.d}/t_{f.s}$ and maximum acceleration.

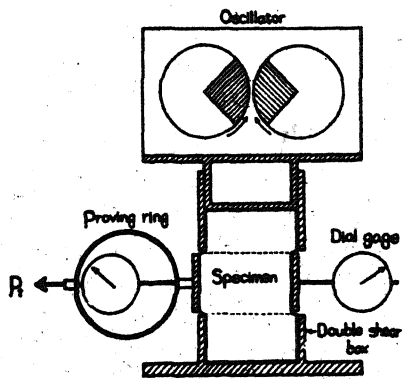


Fig. 15 Dynamic direct double-shear box apparatus.

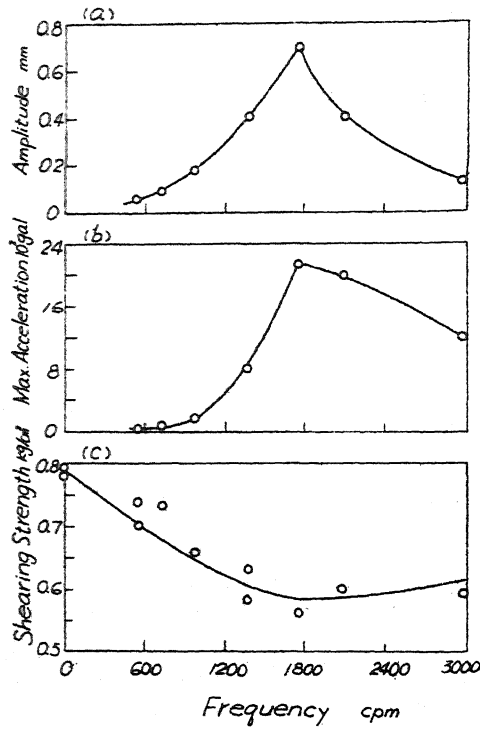


Fig. 16

The results of shearing tests during vibrations. (a) the vertical displacement amplitude, (b) maximum acceleration of vibration and (c) shearing strength during vibration are plotted against the frequency.

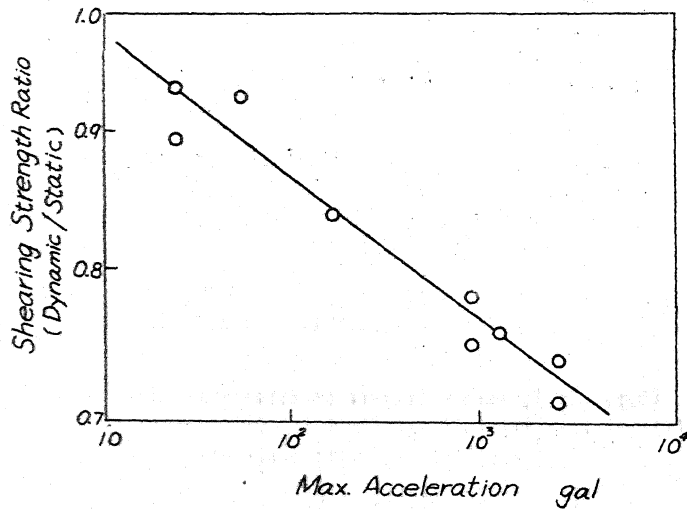


Fig. 17

Relationship between the ratio of the shearing strength in dynamic case to that in static one and the maximum acceleration.